Impingement factor in the case of phase transformations governed by spatially correlated nucleation

M. Tomellini
Dipartimento di Scienze e Tecnologie Chimiche, Università di Roma Tor Vergata, Via della Ricerca Scientifica, 00133 Roma, Italy

M. Fanfoni
Dipartimento di Fisica, Università di Roma Tor Vergata, Via della Ricerca Scientifica, 00133 Roma, Italy
(Received 18 March 2008; revised manuscript received 28 May 2008; published 29 July 2008)

The Kolmogorov-Johnson-Mehl-Avrami (KJMA) theory fails to treat nonrandom nucleation and overgrowth processes. However, the very tractability of their solution in describing experimental data caused researchers to slightly modify KJMA's differential equation so as to extend the applicability of the model. In doing this a phenomenological parameter is introduced, named as the impingement factor. Here we analyze, in depth, the limits within which the phenomenological approach is suitable for sidestepping the difficulty of nonrandom nucleation. In particular we tackled two cases: instantaneous cluster growth where cluster overgrowth prevails and the constant nucleation rate of spatially correlated nuclei according to the hard-core model. In the last part of the paper we show that Avrami's general set theory is equivalent to the statistical mechanics of rigid disks. This permits a deeper appreciation of the KJMA theory and the nonrandom nonsimultaneous kinetics.

DOI: 10.1103/PhysRevB.78.014206 PACS number(s): 68.55.A−, 81.10.Aj, 05.70.Fh, 81.15.Aa

I. INTRODUCTION

Owing to its simplicity, the theory developed by Kolmogorov, Johnson, Mehl, and Avrami (KJMA) between the end of the 1930s and the beginning of the 1940s has been widely used in materials science for describing phase transformation kinetics occurring via nucleation and growth processes.[1–3] In particular, apart from the early applications to the metallurgy, the theory has been recently applied to study the phase separations in multicomponent alloys,[4] the film growth on solid substrates,[5] the kinetics of Ising lattice-gas model,[6] and the DNA replication,[7] just to cite a few among the many systems studied. For instance, in the case of film growth, the KJMA approach has been employed to determine physical quantities such as the film roughness, the autocorrelation function, and the perimeter of the deposit.[5,8,9] Moreover, significative advancement has been done in the ambit of numerical approaches which permit to obtain information on the morphology of the system as well as to check the reliability of the KJMA kinetics for modeling systems which are not consistent with the theoretical premises of the theory.[10–16] In fact, the applicability of the theory is subjected to some conditions. The most peculiar concerns the nucleation phenomena that are required to be Poissonian throughout the whole space where the transition takes place. It is this very assumption that allows the time dependence of transformed phase to be determined analytically.[1] As far as the growth law is concerned, the KJMA model does not deal with the anisotropic growth of the nuclei (which gives rise to the so-called shielding effect)[14,17,18] as well as with growth laws where "phantom overgrowth" is permitted.[19,20] In addition, the growth law has to be the same for all nuclei and the phase transition occurs homogeneously throughout the sample; i.e., the system has to be translationally invariant.[21] It is not surprising that together with many real systems that satisfy the KJMA assumption, there exist as many that do not. In these cases the kinetics not only deviate from the KJMA one but also change substantially, among others, the island size distribution function and the kinetics of number of islands. This is due basically to the different mechanism of nucleation and growth as it occurs in thin-film growth [two dimensional (2D)]. A sharp example of the difference between the island size distribution function is given in the work of Farjas and Roura,[22] based on KJMA approach, as compared with that of Mulheran and Blackman,[23] based on Voronoi tessellation.

In the middle of 1950s, in an attempt to yield a more general kinetic expression, a phenomenological equation was proposed.[24,25] The idea is to introduce a parameter, β, in the 2D KJMA expression (the extension to any spatial dimension is straightforward) as follows:

$$\frac{dS}{dS_e} = (1 - S)^{\beta}, \tag{1}$$

where S is the fraction of the transformed phase and S_e is the extended surface of the new phase (see below). For $\beta=1$ Eq. (1) reduces to the KJMA equation, while for $\beta=2$ it reduces to the Austin-Rickett (AR) equation[26] that is expected to hold in the case of film growth in high supersaturation environment. It is worth citing that Eq. (1) recently has been shown to be suitable for describing several precipitation reactions.[4,27] Usually S_e is taken as a phenomenological power law, i.e., $S_e=Kt^n$, where t is the running time and K and n are constants, with the latter called as Avrami's exponent. Nevertheless, it is important to underline that the definition of extended surface, in the spirit of Avrami's definition, where nucleation centers exist until the beginning of the transition, is the total surface of the new phase independent of the overlaps among clusters arising by all the *allowed* nucleation events. An example of spatially correlated nucleation is displayed in Fig. 1. In particular it refers to a hard-core correlation among nuclei; that is, nucleation events are not permitted within a circle of radius R_{hc} concentric with a nucleus.

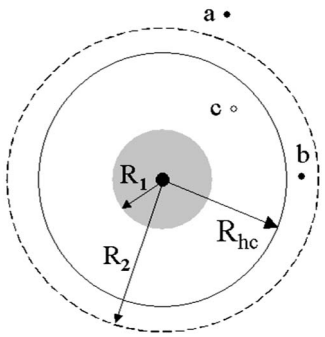

FIG. 1. Schematic representation of *allowed* nucleation centers. Dots a and b are both possible nucleation centers. In the figure two configurations are shown for cluster radii R_1 and R_2. For $R=R_2$ the pre-existing nucleation center b might become a phantom nucleus, while a has a chance to start growing. Because of the correlation ($R=R_{hc}$), no nuclei can lay within the correlation zone; i.e., a nucleation event at c is not allowed.

Recently a detailed study on the breakdown of the KJMA assumptions and its effect on the value of both the impingement factor and Avrami's exponent in kinetics equation (1) has been performed.[27] This survey deals with several possible mechanisms which cause the transformation kinetics to deviate from the KJMA description. Analysis of each single mechanism, separately, also made it possible (by means of the superposition of Gaussian distributions) to estimate the contribution of each mechanism to the experimental kinetics. The breakdown of the KJMA hypothesis considered in Refs. 21 and 27 includes, for example, inhomogeneity of the sample, growth rates that vary with time and space, and transformation with anisotropic growths. In all these cases, however, the nucleation process is still taken as Poissonian—or locally Poissonian in the case of inhomogeneous systems—in the whole space. In other words, the KJMA requirement of random nucleation process is assumed to hold. However, the Poissonian distribution of nuclei is certainly not fulfilled in thin-film growth where two nuclei cannot be formed at relative distance less, on average, than the monomer diffusion length;[5] i.e., nucleation is a non-Poissonian process. This was shown, experimentally, through the measurements of the pair-correlation function as done in Ref. 28. Moreover, even in the three-dimensional (3D) case, an example exists concerning nonrandom nucleation as in the process of primary crystallization.[20] Several cases on nonuniform random nucleation have been studied by employing probability theory[29] and numerical simulations.[30] It is worth reminding that Avrami in his 1939 celebrated paper in fact provided the series expansion describing, formally, any kinetic transition whatever the nucleation process is.

In this paper we deal with nonuniform nucleation in two dimensions, which, as reported above, is of particular interest in film growth. For reasons that will soon be clear, the β parameter is written as $\beta=1-\gamma$, where γ is the "impingement factor."

In this paper: (i) we discuss the meaning of the impingement factor in the case of spatially correlated nucleation for both instantaneous growth and continuous nucleation rate; and (ii) we bridge the gap between Avrami's set theory and the statistical mechanics of rigid disks. This permits us to give an assessment of the possible interpretation of the AR equation based on the non-Poissonian nature of the nucleation process. Our study shows that the γ value depends on the nucleation and growth mode; that is, the impingement factor can be used to characterize the phase transformation typology.

The paper is divided as follows: Section II deals with phase transitions ruled by the instantaneous growth, where any modeling based on the KJMA theory fails. Section III is devoted to the case of spatially correlated nuclei, where the kinetics is ruled by constant nucleation rate and linear growth law. Section IV is concerned on the connection between Avrami's set theory and the statistical thermodynamics of rigid disks.

II. PHASE TRANSITIONS RULED BY INSTANTANEOUS GROWTH

This section deals with transformation in which each nucleus, once nucleated, grows instantaneously to a given constant size R. This peculiar growth mode is of importance in the formation of multilayer structures and interfaces as reported in Ref. 31 (and references therein). It is apparent that under these circumstances the KJMA theory does not apply because of the overgrowth of the phantom nuclei.[19,31] To investigate the meaning of the impingement factor, we first solve the kinetic problem and then compare its solution with that obtained by using Eq. (1). On the basis of the above-mentioned definition of S_e, we get

$$S_e(t) = N(t)\pi R^2, \tag{2}$$

where R is the nucleus radius, $N(t)$ is the number density of actual nuclei, i.e., the number of nucleation events. The solution of Eq. (1) therefore reads ($\gamma \neq 1$; $\gamma \neq 0$; $\gamma S_e \leq 1$)

$$S = 1 - (1 - \gamma S_e)^{1/\gamma}. \tag{3}$$

The same problem can be solved exactly by employing the statistical method based on the correlation functions. In fact, the nucleation being prohibited within an already transformed region, the nuclei turn out to be spatially correlated. The fraction of the transformed phase, $S(t)$, can be written following the theory of Kolmogorov[1] as

$$S(t) = 1 - Q(t), \tag{4}$$

where $Q(t)$ is the probability that the domain Δ_R, namely, a circle of radius R, is empty of nucleation centers. This probability has been computed by several authors[32–34] in terms of either n-particle distribution functions or n-particle correlation functions. Here, we report three expressions for this probability that will be employed throughout the paper. These probabilities prove to be functions of time as the nucleus density depends on time; they are

$$Q(\Delta_R) = 1 + \sum_{m=1}^{\infty} \frac{(-1)^m}{m!} \int_{\Delta_R} f_m(\mathbf{r}_1, \ldots, \mathbf{r}_m) d\mathbf{r}_1 \cdots d\mathbf{r}_m, \tag{5}$$

$$Q(\Delta_R) = 1 + \sum_{m=1}^{\infty} \frac{(-1)^m}{m!} \int f_m(\mathbf{r}_1, \ldots, \mathbf{r}_m)\Omega_m(\mathbf{r}_1, \ldots, \mathbf{r}_m) \times d\mathbf{r}_1 \cdots d\mathbf{r}_m, \tag{6}$$

$$Q(\Delta_R) = \exp\left[\sum_{m=1}^{\infty} \frac{(-1)^m}{m!} \int_{\Delta_R} g_m(\mathbf{r}_1, \ldots, \mathbf{r}_m) d\mathbf{r}_1 \cdots d\mathbf{r}_m\right], \tag{7}$$

where $f_m(\mathbf{r}_1, \ldots, \mathbf{r}_m)$ is the m-dot distribution function, $g_m(\mathbf{r}_1, \ldots, \mathbf{r}_m)$ is the m-dot correlation function, and $\Omega_m(\mathbf{r}_1, \ldots, \mathbf{r}_m)$ is the total area (per unitary surface) of overlap of m disks of radius R when their centers are at the stated positions. If not stated explicitly, integration is intended over the entire space. It goes without saying that Eqs. (5)–(7) can be similarly employed to evaluate the probability of having no nuclei in a circle of generical radius X, which can also be a function of time.

The m-dot correlation functions are related to the m-dot distribution functions by the following cluster expansion:[34]

$$f_m(\mathbf{r}_1, \ldots, \mathbf{r}_m) = \sum_{\mathbf{n}} \sum_{P} [g_1]^{n_1}[g_2]^{n_2} \cdots [g_m]^{n_m}, \tag{8}$$

where the components of the vector $\mathbf{n}$ satisfy the condition $\Sigma_k k n_k = m$ and P indicates that only the distinct contributions arising from the permutation of the m variables $\mathbf{r}_1, \ldots, \mathbf{r}_m$ in the product of the g's have to be retained in the sum. The first two distribution functions are given by

$$f_1(\mathbf{r}_1) = g_1(\mathbf{r}_1), \tag{9}$$

$$f_2(\mathbf{r}_1, \mathbf{r}_2) = g_1(\mathbf{r}_1)g_1(\mathbf{r}_2) + g_2(\mathbf{r}_1, \mathbf{r}_2). \tag{10}$$

In order to check the worth of the phenomenological approach, it is convenient to expand Eq. (3) in Taylor's series and to compare it with the exact expansion occurring in Eq. (5). Equation (3) then becomes

$$Q = 1 + \sum_{n=1}^{\infty} \frac{(-1)^n}{n!} a_n S_e^n, \tag{11}$$

where $a_n = [1-(n-1)\gamma]a_{n-1}$ and $a_0 = 1$. However, before comparing the two series, some considerations on Eq. (5) are in order.

In fact, Eq. (5) is equal to the fraction of surface that is not covered by the disks. On the basis of geometrical considerations, it is clear that if all distances transform according to $X \to \lambda X$, then $N \to N/\lambda^2$, where λ is the scaling parameter. Naturally the $Q(\Delta_R)$ is invariant under such a transformation. In other words, this probability is a zero-order homogeneous function in λ. Consequently $Q(\Delta_R)$ is expected to be a function of $S_e = N\pi R^2$ (see also the Appendix).

However, one must bear in mind that, although for the problem at hand only terms up to $m=5$ contribute to the sum [Eq. (5)]—in fact the requirement of finding m dots within the circle of radius R cannot be satisfied for $m>5$; i.e., $f_{m>5}=0$ in this domain[35]—Eq. (5) is a power series of S_e. For instance, the radial distribution function of hard disks, $g(\mathbf{r}_1, \mathbf{r}_2) = \frac{f_2(\mathbf{r}_1, \mathbf{r}_2)}{N^2}$, is in the form

$$g(\xi) = H(\xi - R)\left[1 + \sum_{n=1}^{\infty} N^n c_n(\xi, R)\right], \tag{12}$$

where $H(x)$ denotes the Heaviside function, $\xi = |\mathbf{r}_1 - \mathbf{r}_2|$, and the system is assumed to be homogeneous and isotropic. In Eq. (12) the sum runs over all $(n+2)$-dot connected diagrams $[c_n(\xi, R)]$, where the integration is carried out over the dots $\mathbf{r}_3, \mathbf{r}_4, \ldots, \mathbf{r}_n$. Furthermore, since for a system of hard disks, $c_n(\xi, R)$ terms are reduced to $2n$-dimensional integrals over the areas of n overlapping disks, these terms will scale as $c_n \propto R^{2n}$. It turns out that $g(\xi)$ is also a power series of the extended surface.

In the case of a homogeneous system, $f_1 = N$ and the evaluation of the term $m=1$ in Eq. (5) is just equal to $-S_e$. As far as the term $m=2$ is concerned, we evaluate only the contribution of the lowest term of the diagrammatic expansion in Eq. (12). From Eq. (5) one attains

$$\frac{1}{2}\int_{\Delta_R} f_2(\mathbf{r}_1, \mathbf{r}_2) d\mathbf{r}_1 d\mathbf{r}_2 = \frac{N^2}{2}\int_{\Delta_R} H(|\mathbf{r}_1 - \mathbf{r}_2| - R) d\mathbf{r}_1 d\mathbf{r}_2, \tag{13}$$

where the integration domain is the circle of radius R. Since both $\mathbf{r}_1$ and $\mathbf{r}_2$ have to lie in this circle, it follows that $\int_{\Delta_R}[1 - H(\xi - R)]d\mathbf{r}_1 d\mathbf{r}_2 = 2\pi\int_0^R r dr A(r, R)$, where $A(r, R)$ is the overlap area of two disks of radius R at relative distance r. This integral is easily calculated as

$$\begin{aligned} &\int_{\Delta_R} [1 - H(\xi - R)] d\mathbf{r}_1 d\mathbf{r}_2 \\ &= 2\pi \int_0^R r dr 4R^2 \int_{r/2R}^1 \sqrt{1 - y^2} dy \\ &= 8\pi R^4 \int_0^1 z dz \int_{z/2}^1 \sqrt{1 - y^2} dy \\ &= \left(1 - \frac{3^{3/2}}{4\pi}\right)(\pi R^2)^2. \end{aligned} \tag{14}$$

By equating the terms of order S_e^2 in the two series, Eqs. (5) and (11), makes it possible, for the problem studied in this section, to identify the impingement factor with the term

$$\gamma = \gamma_0 = \left(1 - \frac{3^{3/2}}{4\pi}\right) \equiv -\frac{1}{S_e^2}\int_{\Delta_R} g_2^{(0)}(\mathbf{r}_1, \mathbf{r}_2) d\mathbf{r}_1 d\mathbf{r}_2, \tag{15}$$

or

$$\beta \equiv \frac{1}{S_e^2}\int_{\Delta_R} f_2^{(0)}(\mathbf{r}_1, \mathbf{r}_2) d\mathbf{r}_1 d\mathbf{r}_2, \tag{16}$$

where the superscript indicates the lowest-order terms and the following relation was employed: $g_2^{(0)}(\xi) = N^2[H(\xi - R) - 1]$. The numerical value of γ computed here, γ_0, coincides with that derived in Ref. 31 by employing a different method. Specifically, in this work the impingement factor is introduced to account for phantom overgrowth which, in this context, is related to the overlap between *actual* and *phantom* nuclei. Our computation shows that the phenomenologi-

cal parameter β entering Eq. (1) acquires a remarkable meaning, being connected to the pair-correlation function of the *actual* nuclei which is different from zero. The question now arises as to the exactness of solution (3) for $\gamma=\gamma_0$. To answer this question, one should compute the higher-order terms of the expansion and compare them to those of Eq. (11). However, this is a very difficult, not to say impossible task since even the computation of the low-order term at $m=3$ requires the knowledge of the three-dot distribution function, for which no exact analytic expression is available. Even the approximate expression based on Kirkwood's superposition assumption leads to a quite complex computation that, in the end, is not reliable for establishing the correctness of Eq. (11). We have therefore adopted a different approach by exploiting the statistical implications of Eq. (3) to deal with a different but better understood process: the random sequential adsorption (RSA). It consists of throwing disks of radius R on a surface where overlaps among them are not permitted.[35–37] The rate at which disks are deposited on the surface is proportional to the probability that a landing disk finds enough room to accommodate itself without overlapping other disks, i.e., the probability of finding a circle of radius $\sigma=2R$ empty of disk centers. The adsorption rate then becomes

$$\frac{dN}{dt} = JQ_\sigma(\Delta_\sigma), \tag{17}$$

where N is the number density of adsorbed disks, J is the flux of incoming disks on the surface, and the subscript of Q indicates the "hard-core" radius (σ). Furthermore, the Q probability, thanks to Eq. (3), is

$$Q_\sigma(\Delta_\sigma) = [1 - \gamma_0(N\pi\sigma^2)]^{1/\gamma_0}, \tag{18}$$

and the adsorption rate becomes

$$\frac{dN}{dt} = J[1 - (4N\pi R^2)\gamma_0]^{1/\gamma_0}. \tag{19}$$

By recalling that in the RSA $S=S_e=N\pi R^2$, it follows that

$$\frac{dN}{dt} = J(1 - 4S\gamma_0)^{1/\gamma_0}, \tag{20}$$

which implies the jamming point ($\frac{dN}{dt}=0$) $S_\infty=\frac{1}{4\gamma_0}=0.426$. The latter differs from the value obtained in the literature for ordinary RSA of identical disks: $S_\infty=0.542$ (Ref. 37) and $S_\infty=0.547$.[38,39] On this basis, we conclude that series expansion (11) is not the exact solution of the kinetics. Nevertheless, on the basis of Monte Carlo simulations, it was shown in Ref. 40 that Eq. (11) is indeed an excellent approximation. This can also be appreciated by studying the RSA kinetics in the coverage domain. To this end Eq. (20) is compared in Fig. 2 to the numerical kinetics in Ref. 35 at unitary J; as it appears the agreement between the two kinetics is excellent. Also shown in the same figure are the kinetics computed by using the probability functions given through Eqs. (5) and (7) by retaining terms up to the second order in both distribution and correlation functions and where only the Heaviside contribution to the radial distribution function has been considered. In the first case, the kinetics is $Q_\sigma(\Delta_\sigma)=1-N\pi\sigma^2+\frac{1}{2}\int_{\Delta_\sigma} f_2^{(0)} d\mathbf{r}_1 d\mathbf{r}_2 = 1-4S+8(1-\gamma_0)S^2$, where $\sigma=2R$. Also displayed in the same figure is the approximate kinetics $\frac{dN}{dt} \propto \exp[-4S(1+2S)]$, which was derived in Ref. 34 by decoupling the integral of the pair-correlation function in Eq. (7).

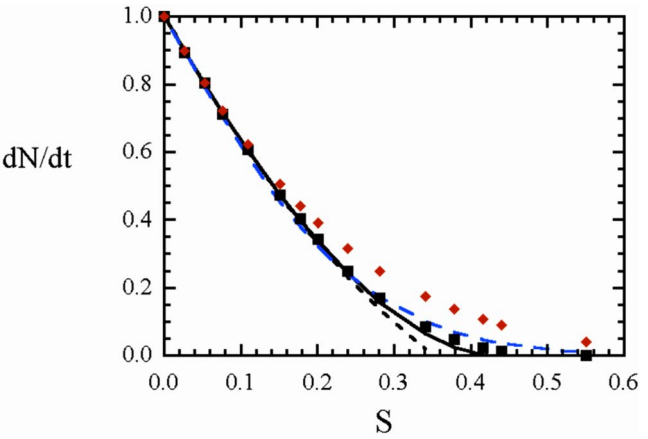

FIG. 2. (Color online) Kinetics of random sequential adsorption of rigid disks in the coverage domain. The adsorption rates dN/dt, as obtained by numerical simulation, are shown as full squares. The behavior of kinetics equation (20), in terms of the impingement factor, is reported as a solid line. The short dashed line is the approximate solution computed by means of the f-series expansion, Eq. (6), up to the second-order term. The diamond symbols (in red) show the kinetics computed by using the correlation functions, Eq. (7), up to the second-order term in the argument of the exponential. In this expansion the lowest-order term of the two-dot correlation function has been retained. The approximate kinetics obtained by decoupling the integrals on the pair-correlation function is also displayed as a long dashed line (blue).

III. CONSTANT NUCLEATION RATE AND LINEAR GROWTH

In this section we deal with spatially correlated nuclei according to the hard-core model; i.e., the distance between two nuclei cannot be shorter than R_{hc}. The growth law of cluster is considered to be linear and the nucleation rate constant. Under these hypotheses the kinetics has been solved, analytically, in Refs. 41 and 42. In this case the stochastic theory requires the definition of different classes of dots (at odds with the simultaneous nucleation case) corresponding to different nucleation times and, in turn, to different sizes of the nuclei.[41] Furthermore, in order to obtain a manageable analytical expression, some approximations have been employed and their validity has been tested by means of Monte Carlo simulations. Also in this case, owing to the correlation among nuclei, the kinetics is given in terms of the extended surface S_e. In the case of constant nucleation rate, $S_e=\frac{1}{3}I\pi a^2 t^3$, with $R(t)=at$ as the nucleus growth law and I as the nucleation rate. In addition, since the nucleation process is not simultaneous, even in this case some dots can be captured by the growing phase, becoming "phantom" clusters. According to Refs. 41 and 42, the solution of the kinetics reads

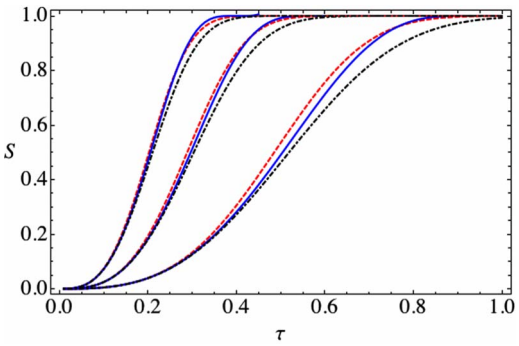

FIG. 3. (Color online) Fraction of transformed surface in the case of correlated nucleation (solid lines) as a function of the dimensionless time τ and for several values of the η parameter. The nucleation and growth rates are constants. Each of the three bunches of curves displays the KJMA solution [Eq. (23); black dashed-dotted lines), phenomenological equation (3) (blue solid lines), and the exact kinetics [Eq. (22); red dashed lines]. From right to left, the parameter values of each bunch are: (a) $\eta=1$, $\gamma=0.25$; (b) $\eta=5$, $\gamma=0.2$; and (c) $\eta=15$, $\gamma=0.2$.

$$\ln(1-S) = -S_e\left\{1+\frac{S_e}{2}H\left(1-\frac{3S_e}{S^*}\right) + \frac{1}{2}\left[S^* - 2S_e\left(\frac{S^*}{3S_e}\right)^{3/2}\right]H\left(\frac{3S_e}{S^*}-1\right)\right\}, \quad (21)$$

where $S^*=\pi R_{\mathrm{hc}}^2 It$ and $H(x)$ is the Heaviside function. Furthermore, let us define the new variables $\eta=S_e/S^{*3}$, $\tau=S^*\gamma_0$, and $S_e=\eta(\frac{\tau}{\gamma_0})^3$, where γ_0 is the impingement factor in Sec. II. The reason for these variables will be clear shortly. Equation (21) then becomes

$$\ln(1-S) = -\frac{\eta\tau^3}{\gamma_0^3}\left[1+\frac{\eta\tau^3}{2\gamma_0^3}H\left(1-3\frac{\eta\tau^2}{\gamma_0^2}\right) + \left(\frac{\tau}{2\gamma_0}-\frac{1}{\sqrt{27\eta}}\right)H\left(3\frac{\eta\tau^2}{\gamma_0^2}-1\right)\right]. \quad (22)$$

We stress that here τ is the dimensionless time variable, whereas η and γ_0 are parameters. The correlated nucleation process discussed so far assumes a constant nucleation rate I during the whole phase transition. This requirement gives rise to a constraint on the value of the η quantity. In fact, to ensure a constant value of I, the "hard disk" fractional coverage at the end of the transition (say, at $t=t_F$), namely, $\pi\frac{R_{\mathrm{hc}}^2}{4}It_F$, has to be lower than the jamming limit: $S_\infty\simeq 0.55$. This condition implies $S^*(t_F)\leq 4S_\infty\simeq 2.2$ and, consequently, $\eta > S_e(t_F)/(4S_\infty)^3$. We also observe that by using the approximate jamming point $S_\infty=\frac{1}{4\gamma_0}$, the condition $S^*(t_F)\leq 4S_\infty$ reduces to $\tau_F\leq 1$, which makes it clear that in this dimensionless variable the kinetics is confined within $\tau\in[0,1]$. For a Poissonian nucleation, $S^*=0$ and Eq. (21) give the KJMA kinetics

$$\ln(1-S) = -S_e. \quad (23)$$

The kinetics computed by means of Eq. (22) is displayed in Fig. 3 as a function of τ and for various η parameters ranging between 1 and 15. In the same figure, the kinetics computed in the case of a Poissonian nucleation [Eq. (23)] is also been shown for comparison. The behavior of these curves is consistent with previous analytical and numerical computations.[41]

Although Eq. (3) has been successfully used for describing the instantaneous growth, here we attempt to use it to describe the kinetics of the correlated system (Fig. 3). To this end we choose a suitable value of the impingement parameter γ by trial and error. The results of this approach are shown in Fig. 3. The description of the kinetics appears to be better the larger the η value is. In particular for η values in the wide interval 1–15, the γ parameter ranges from 0.2 to 0.3. In addition, the impingement parameter exhibits a weak dependence on η, namely, $\gamma\simeq 1.34\eta^{-0.047}$. In practice, in this interval the impingement factor can be considered constant provided the kinetics is expressed in the dimensionless variables defined above. The KJMA curve is recovered in the limit $\eta\to\infty$.

Before concluding this section, we propose a different approach to the determination of the kinetics of growth in the case of hard-core correlated nucleation. It is based on the concept of phantom nuclei.

It is well known that nucleation centers scattered at random throughout the whole surface are distributed by Poisson's statistics.[1] This is not true in the case of hard-core correlated nucleation since nucleation is forbidden within nucleation circles (centered at a nucleation site) of radius R_{hc}. Nevertheless it is possible to estimate from $I(t)$, that is, the rate of the allowed nucleation events, what would be the nucleation rate in the absence of nucleation constraints; it is

$$I_P(t) = \frac{I(t)}{1-S_c(t)}, \quad (24)$$

where $S_c(t)$ is the fraction of surface area prohibited to the nuclei at time t. As a matter of fact, this surface can be easily computed by resorting to the previous results and by considering that the number of clusters formed up to t (phantom included) is $N(t)=\int_0^t I(t')dt'$ and $R\equiv R_{\mathrm{hc}}$. For a constant nucleation rate, $I(t)=I$ and $N(t)=It$. In addition, we employ Eq. (3) with $\gamma=\gamma_0$ for estimating the $S_c(t)$ kinetics. Equation (24) becomes

$$I_P(t) = \frac{I}{(1-\gamma_0 I\pi R_{\mathrm{hc}}^2 t)^{1/\gamma_0}}. \quad (25)$$

The next step of our approach is to determine the "Poissonian extended surface,"

$$\begin{aligned} S_{eP}(t) &= \pi a^2\int_0^t I_P(t')(t-t')^2dt' \\ &= \pi a^2\int_0^t \frac{I}{(1-\gamma_0 I\pi R_{\mathrm{hc}}^2 t')^{1/\gamma_0}}(t-t')^2dt' \\ &= \frac{3\eta}{\gamma_0^3}\int_0^\tau \frac{(\tau-\tau')^2}{(1-\tau')^{1/\gamma_0}}d\tau', \end{aligned} \quad (26)$$

that can be integrated to give

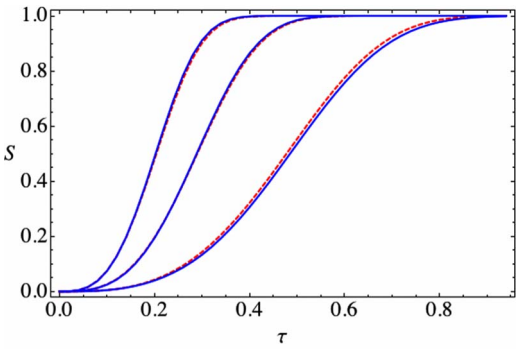

FIG. 4. (Color online) Modeling the phase transition in the case of nonrandom nucleation by employing the Poissonian extended surface in the KJMA expression. The nucleation and growth rates are constants. The exact solutions are displayed as solid lines (blue); the dashed lines are the kinetics computed in the framework of the Poisson process, i.e., KJMA approach. From right to left, the parameter values of each bunch are: (a) $\eta=1$, (b) $\eta=5$, and (c) $\eta=15$.

$$S_{eP}(\tau) = \frac{3\eta}{\gamma_0^3}\left\{\frac{\tau}{b_1}\left(\tau - \frac{2}{b_2}\right) + \frac{2}{b_1 b_2 b_3}[1-(1-\tau)^{b_3}]\right\}, \tag{27}$$

where $b_n = \frac{n\gamma_0 - 1}{\gamma_0}$. We therefore compute the fractional surface coverage by resorting to the Poissonian process, i.e., the KJMA theory, according to

$$S(t) = 1 - \exp[-S_{eP}(t)], \tag{28}$$

which has to be compared with the "exact" solution [Eq. (22)]. It is clear that the two kinetics are expected to coincide provided all the *extra* nucleation centers introduced into the forbidden area $S_c(t)$ (for example, the c nucleus in Fig. 1) are phantoms. Since this is not strictly true, Eq. (28) is an approximation. Its merit is checked in Fig. 4, where it can be seen that for $\eta > 1$ the approximation is very good. Nevertheless, in the framework of the hard-core model, the constant nucleation process is allowed, during the whole transition, provided $\eta > 1$. One then concludes that solution (28) is an excellent approximation for the transition ruled by the non-Poissonian nucleation presented here.

In addition, in the limit $\eta \to \infty$ and $\tau \to 0$, Eq. (28) leads to the KJMA kinetics, Eq. (23). This is easily seen by studying the behavior of Eq. (27) at low τ values. In fact, Taylor's expansion of this equation provides $S_{eP} \simeq \frac{\eta\tau^3}{\gamma_0^3} = \frac{1}{3}\pi I a^2 t^3$ and Eq. (28) reduces to Eq. (23).

For the sake of completeness, in Figs. 5(A) and 5(B) we show the behavior of Avrami's exponent as computed, analytically, by using Eqs. (27) and (28). Avrami's exponent is defined as usual as the local slope in the graph of $\ln\{-\ln[1-S(\tau)]\}$ vs $\ln(\tau)$, that is, $n(\tau) = \frac{d\ln(S_{eP})}{d\ln(\tau)}$. Panel (A) shows the function $n(\tau)$, which, being independent of η, is in fact a universal function. In panel (B) Avrami's exponent is displayed as a function of surface coverage for (a) $\eta=1$, (b) $\eta=5$, (c) $\eta=15$, and (d) $\eta=100$. This graph evidences that the possibility of describing a strongly correlated system through

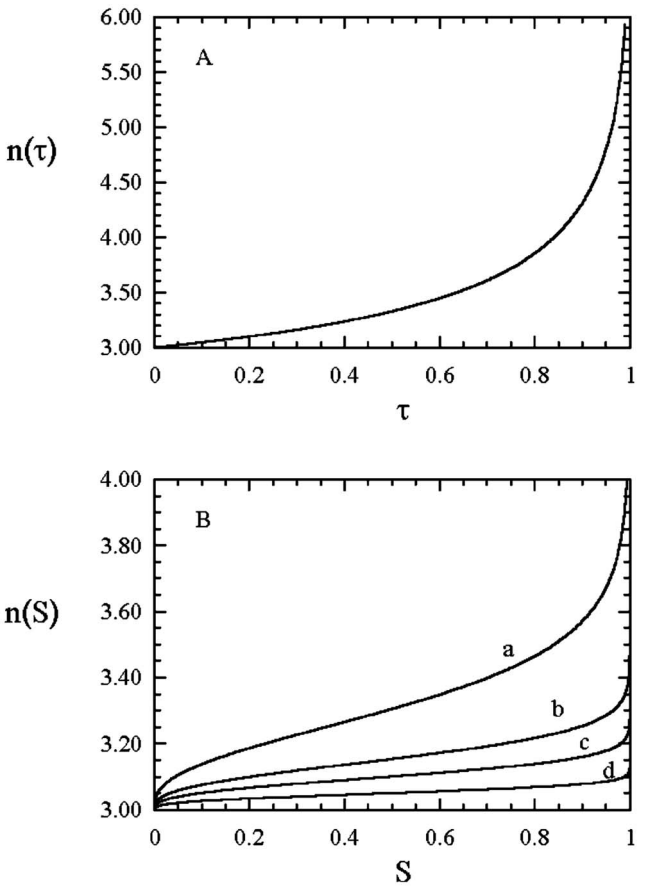

FIG. 5. The Avrami exponent n for the kinetics in Fig. 4 is displayed. In panel (A) n is plotted as a function of τ and it is a "universal" curve. In panel (B) it is plotted as a function of surface coverage for (a) $\eta=1$, (b) $\eta=5$, (c) $\eta=15$, and (d) $\eta=100$. In the limit $\eta \to \infty$, $n=3$.

a single value of Avrami's phenomenological exponent is unrealistic. On the other hand, in the limit of sizable η values, i.e., small R_{hc}, the KJMA curve is approached ($n=3$). It is worth noting that the use of a stretched exponential entails the definition of two phenomenological parameters.

IV. CONNECTION BETWEEN AVRAMI'S SET THEORY AND THE STATISTICAL MECHANICS OF RIGID DISKS

For the sake of completeness, it is worth stressing that Eq. (6) is a particular case of the expression derived by Avrami in his original paper that, for the 2D case, reads[2]

$$1 - S = 1 + \sum_{m=1}^{\infty} (-)^m S_{e,m}, \tag{29}$$

where S is the fraction of transformed surface and $S_{e,m}$ is the extended surface of order m,

$$S_{e,m} = \sum_{k=m}^{\infty} \frac{k!}{m!\,(k-m)!} S'_k, \tag{30}$$

where S'_m is the contribution to the transformed area due to the overlaps between m nuclei. With reference to the kinetics

discussed in Secs. II and III, we stress that $S_e \equiv S_{e,1}$. In the specific case of clusters having the same size, Eq. (6) shows that

$$S_{e,m} = \frac{1}{m!}\int f_m(\mathbf{r}_1, \ \ldots, \mathbf{r}_m)\Omega_m(\mathbf{r}_1, \ \ldots, \mathbf{r}_m)d\mathbf{r}_1 \cdots d\mathbf{r}_m. \tag{31}$$

Since Eq. (29) has been obtained on the basis of purely geometrical arguments, it is of general validity; i.e., it also holds in the case of disk size distribution. Moreover in Avrami's first paper, the extended surfaces entering Eq. (29) were defined without the inclusion of the phantom clusters as we also did in writing Eqs. (5)–(7). However, it can be simply proved that Eq. (29) also holds by including the contribution of phantoms provided the overgrowth process is not permitted.

The generalization of Eq. (31) for dealing with a disk size distribution (nonsimultaneous nucleation) of correlated dots requires the definition of several classes of dots (nucleation centers).[42] Dots with the same birth time belong to the same class and, consequently, give rise to nuclei of the same size. Let us define the m-dot distribution function as $f^{(m)}_{ijk\ldots}(\mathbf{r}_{1,i}, \mathbf{r}_{2,i}, \ \ldots, \mathbf{r}_{m_i,i}, \mathbf{r}_{1,j}, \mathbf{r}_{2,j}, \ \ldots, \mathbf{r}_{m_j,j}, \mathbf{r}_{1,k}, \ \ldots)$, where $i,j,k, \ \ldots$ denote the classes of dots and $m_i+m_j+m_k+\cdots=m$ is the number of dots being larger, or equal, to the number of classes. Furthermore we denote with $\Omega^{(m)}_{ijk\ldots}(\mathbf{r}_{1,i}, \mathbf{r}_{2,i}, \ \ldots, \mathbf{r}_{m_i,i}, \mathbf{r}_{1,j}, \mathbf{r}_{2,j}, \ \ldots, \mathbf{r}_{m_j,j}, \mathbf{r}_{1,k}, \ \ldots)$ the total area (per unitary surface) of overlap of the m disks of radius $R_i, R_j, R_k, \ \ldots$ when their centers are at the stated positions. The first-order term in Eq. (29) becomes

$$S_{e,1} = \sum_i N_i \int \Omega^{(1)}(\mathbf{r}_i)d\mathbf{r}_i = \sum_i N_i s_i, \tag{32}$$

where s_i is the disk area and N_i is the surface density of dots. In this last equation we made use of the relation $f^{(1)}_i(\mathbf{r}_i)=N_i$, which holds in the case of a homogeneous system. The second-order term in Eq. (29) is attained by considering the contribution arising from all the distinct couples of dots,

$$S_{e,2} = \frac{1}{2}\sum_i \int f^{(2)}_{ii}\Omega^{(2)}_{ii}d\mathbf{r}_{1,i}d\mathbf{r}_{2,i} + \sum_{i>j}\int f^{(2)}_{ij}\Omega^{(2)}_{ij}d\mathbf{r}_{1,i}d\mathbf{r}_{2,j}, \tag{33}$$

where the short notation $\Omega^{(2)}_{ij}=\Omega^{(2)}(\mathbf{r}_{1,i}, \mathbf{r}_{2,j})$, $f^{(2)}_{ij}=f^{(2)}(\mathbf{r}_{1,i}, \mathbf{r}_{2,j})$ was used. Equation (33) can be rewritten in the form

$$S_{e,2} = \frac{1}{2}\sum_{i,j}\int f^{(2)}_{ij}\Omega^{(2)}_{ij}d\mathbf{r}_{1,i}d\mathbf{r}_{2,j}. \tag{34}$$

In like manner, the computation of the third-order term leads to

$$S_{e,3} = \frac{1}{2!}\sum_{i\neq j}\int f^{(3)}_{iij}\Omega^{(3)}_{iij}d\mathbf{r}_{1,i}d\mathbf{r}_{2,i}d\mathbf{r}_{3,j} + \sum_{i>j>k}\int f^{(3)}_{ijk}\Omega^{(3)}_{ijk}d\mathbf{r}_{1,i}d\mathbf{r}_{2,j}d\mathbf{r}_{3,k} + \frac{1}{3!}\sum_i\int f^{(3)}_{iii}\Omega^{(3)}_{iii}d\mathbf{r}_{1,i}d\mathbf{r}_{2,i}d\mathbf{r}_{3,i}, \tag{35}$$

which is rewritten according to

$$S_{e,3} = \frac{1}{3!}\sum_{i,j,k}\int f^{(3)}_{ijk}\Omega^{(3)}_{ijk}d\mathbf{r}_{1,i}d\mathbf{r}_{2,j}d\mathbf{r}_{3,k}, \tag{36}$$

where the i,j,k indices run over all classes of dots. Therefore, the extended surface of order m reads

$$S_{e,m} = \frac{1}{m!}\sum_{i_1,i_2,\ \ldots,i_m}\int f^{(m)}_{i_1 i_2\cdots i_m}\Omega^{(m)}_{i_1 i_2\cdots i_m}d\mathbf{r}_{1,i_1}d\mathbf{r}_{2,i_2}\ldots d\mathbf{r}_{m,i_m}, \tag{37}$$

where i_k is the class index.

Equations (29) and (37) give the kinetics in terms of integrals over the m-dot distribution functions and the overlap areas of m disks. However, in analogy to Eq. (5), the kinetics can also be expressed in terms of a series of integrals over the m-dot distribution functions only. One gets

$$1 - S = 1 + \sum_{m=1}^{\infty}\frac{(-1)^m}{m!}\sum_{i_1,i_2,\ \ldots,i_m}\int_{\Delta_{R_{i_1}}} d\mathbf{r}_{1,i_1} \times \int_{\Delta_{R_{i_2}}} d\mathbf{r}_{2,i_2}, \ \ldots, \int_{\Delta_{R_{i_m}}} d\mathbf{r}_{m,i_m} f^{(m)}_{i_1 i_2\cdots i_m}, \tag{38}$$

where the integration domains are now the circles of radii $R_{i_1}, R_{i_2}, \ \ldots, R_{i_m}$. It is worth recalling that starting from Eq. (38) the kinetics can be further expressed in exponential form by means of the cluster expansion of the distribution functions in terms of m-dot correlation functions.[42]

In the case of a Poissonian distribution of dots, Eq. (29), together with Eq. (37), must coincide with the KJMA solution

$$1 - S = 1 + \sum_{m=1}^{\infty}\frac{(-1)^m}{m!}S^m_{e,1} \equiv \exp(-S_{e,1}), \tag{39}$$

which implies $S_{e,m}=\frac{1}{m!}S^m_{e,1}$.

It is instructive to verify that the extended surface of orders 1 and 2 in Eq. (37) actually reduces to $S_{e,1}$ and $\frac{S^2_{e,1}}{2}$, respectively. Furthermore, in the case of circular disks, from Eq. (32),

$$S_{e,1} = \sum_i N_i \pi R_i^2, \tag{40}$$

where R_i is the disk radius.

The equality between the first-order terms of the two series has already been demonstrated by exploiting the homogeneity of the system [Eq. (32)]. As far as the second-order term is concerned ($m=2$), the demonstration reduces to the

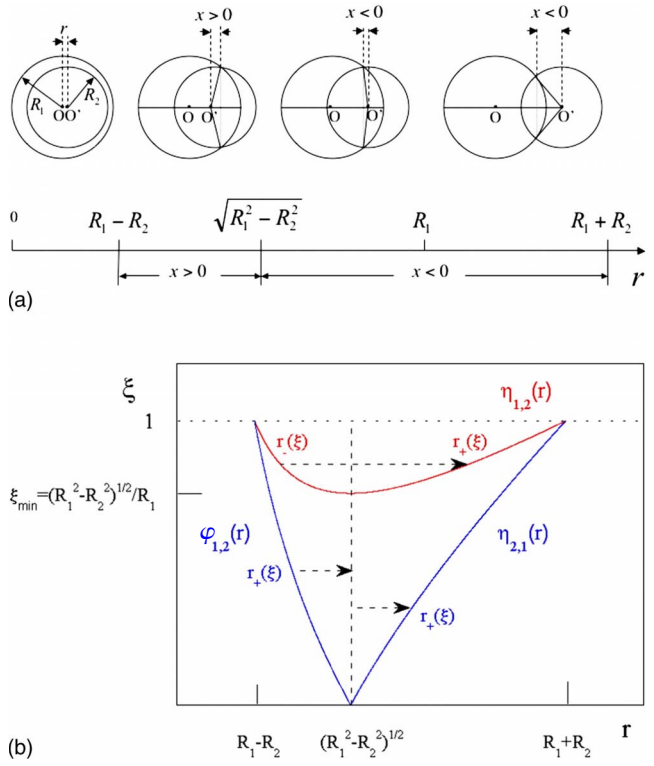

FIG. 6. (Color online) (a) Schematic representation of the configurations of a pair of overlapping disks of radii R_1 and R_2 as a function of relative distance r. The values defining the integration domains of the I_i integrals are also shown. For $r<R_1-R_2$, the smaller nucleus is a phantom. (b) Behavior of the $\eta_{1,2}(r)$, $\eta_{2,1}(r)$, and $\varphi_{1,2}(r)$ functions which enter the I_i integrals. The minimum of the $\eta_{1,2}(r)$ function is marked. The integration paths, after the order of integration has been inverted, are displayed through arrows. The roots of the equations $\xi=\eta_{1,2}(r)$, $\xi=\eta_{2,1}(r)$, and $\xi=\varphi_{1,2}(r)$, required to invert the order of integration, are also shown. Specifically, they are two for $\eta_{1,2}$ and one for both $\eta_{2,1}$ and $\varphi_{1,2}$.

computation of the overlap between two disks of different radii, say, R_1 and R_2, where $R_1>R_2$ is assumed. Since the distribution of dots is random throughout the entire space, then $f_{12}^{(2)}=N_1N_2$ and the computation of Eq. (34) implies the estimate of the integral

$$I_0 = N_1N_2 \int \Omega^{(2)}(\mathbf{r}_1,\mathbf{r}_2)d\mathbf{r}_1d\mathbf{r}_2 = N_1N_2 \int 2\pi r dr A_2(R_1,R_2,r), \tag{41}$$

where $A_2(R_1,R_2,r)$ is the overlap area of the two disks at relative distance r. One observes that I_0 is just proportional to the average value of the overlap area between a pair of disks. A scheme of the typical configurations of two disks, in relation to the relative distance r, is shown in Fig. 6(a). We underline that, since the growth law is linear $[R(t-t')=a(t-t')$, where t' is the birth time of the nucleus], the overgrowth phenomenon does not occur. Let us now consider the transformation of a nucleus in a phantom, that is, the "capture" of a smaller dot (radius R_2) by a larger dot (radius R_1) owing to the growth. In order that the nucleus with radius $R_2=a(t-t_2)$ be a *phantom*, the condition $t_2>\tilde{t}$ has to be fulfilled, where $\tilde{t}$ satisfies the equation $r=a(\tilde{t}-t_1)$, with r as the relative distance between the two nuclei. Therefore, the following inequality holds: $R_2=a(t-t_2)<a(t-t_1)-r=R_1-r$, namely, $r<R_1-R_2$, which means that the second disk (R_2) is completely covered by the first one (R_1). Conversely, a nucleus placed at $r>R_1-R_2$ will never be captured by the first nucleus. It follows that, although r spans the whole interval $0<r<\infty$, the overlap area will be different from zero only in the range $0<r<R_1+R_2$. The area A_2 is estimated according to [see Fig. 6(a)]

$$\begin{aligned} A_2(R_1,R_2,r) = {} & \pi R_2^2 \chi_{0,R_1-R_2}(r) \\ & + \left\{ \pi R_2^2 + 2\left[R_1^2 \int_{\eta_{1,2}(r)}^{1} \sqrt{1-\xi^2}d\xi \right.\right. \\ & \left.\left. - R_2^2 \int_{\varphi_{1,2}(r)}^{1} \sqrt{1-\xi^2}d\xi \right] \right\} \chi_{R_1-R_2,\sqrt{R_1^2-R_2^2}}(r) \\ & + 2\left[R_1^2 \int_{\eta_{1,2}(r)}^{1} \sqrt{1-\xi^2}d\xi \right. \\ & \left. + R_2^2 \int_{\eta_{2,1}(r)}^{1} \sqrt{1-\xi^2}d\xi \right] \chi_{\sqrt{R_1^2-R_2^2},R_1+R_2}(r), \end{aligned} \tag{42}$$

where $\eta_{i,j}(r)=\frac{r}{2R_i}+\frac{R_i^2-R_j^2}{2rR_i}$, $\varphi_{1,2}(r)=\frac{R_1^2-R_2^2}{2rR_2}-\frac{r}{2R_2}$, and the characteristic function $\chi_{a,b}(x)=1$ for $x\in[a,b)$ and $\chi(x)=0$ otherwise. The determination of the mean value of the overlap area reduces to the computation of the following integrals:

$$I_1 = 2\pi \int_{R_1-R_2}^{R_1+R_2} r dr \int_{\eta_{1,2}(r)}^{1} 2R_1^2\sqrt{1-\xi^2}d\xi, \tag{43}$$

$$I_2 = 2\pi \int_{\sqrt{R_1^2-R_2^2}}^{R_1+R_2} r dr \int_{\eta_{2,1}(r)}^{1} 2R_2^2\sqrt{1-\xi^2}d\xi, \tag{44}$$

and

$$I_3 = -2\pi \int_{R_1-R_2}^{\sqrt{R_1^2-R_2^2}} r dr \int_{\varphi_{1,2}(r)}^{1} 2R_2^2\sqrt{1-\xi^2}d\xi. \tag{45}$$

These integrals can be easily solved by inverting the order of integration, which implies the inversion of the $\eta(r)$ and $\varphi(r)$ functions depicted in Fig. 6(b). In particular Eq. (43) reads

$$I_1 = \int_{\xi_{\min}}^{1} 4\pi R_1^2\sqrt{1-\xi^2}d\xi \int_{r_-(\xi)}^{r_+(\xi)} r dr, \tag{46}$$

where $r_+(\xi)$ and $r_-(\xi)$ $(r_+>r_-)$ are the two roots of the equation $\xi=\eta_{1,2}(r)$ and $\xi_{\min}=\frac{(R_1^2-R_2^2)^{1/2}}{R_1}$ [Fig. 6(b)]. The I_1 integral then becomes

$$I_1 = 8\pi R_1^4 \int_{\xi_{\min}}^{1} \xi\sqrt{1-\xi^2}\sqrt{\left(\frac{R_2}{R_1}\right)^2-(1-\xi^2)}d\xi. \tag{47}$$

Following a similar computation pathway, the other two integrals can be recast in the form

$$I_2 = 4\pi R_2^4 \int_0^1 \sqrt{1-\xi^2}\left\{\xi\sqrt{\left(\frac{R_1}{R_2}\right)^2 - (1-\xi^2)} + \xi^2\right\} d\xi \tag{48}$$

and

$$I_3 = -4\pi R_2^4 \int_0^1 \sqrt{1-\xi^2}\left\{\xi\sqrt{\left(\frac{R_1}{R_2}\right)^2 - (1-\xi^2)} - \xi^2\right\} d\xi. \tag{49}$$

The evaluation of I_0 eventually reduces, with $I_1 = I_2 + I_3 = \frac{\pi^2}{2} R_2^4$, to

$$I_0 = N_1 N_2 \{I_1 + I_2 + I_3 + \pi^2 R_2^2 (R_1 - R_2)^2 + \pi^2 R_2^2 [R_1^2 - R_2^2 - (R_1 - R_2)^2]\} = N_1 N_2 \pi^2 (R_1 R_2)^2. \tag{50}$$

Specifying Eq. (50) in Eq. (34), one ends up with the expected result

$$S_{e,2} = \frac{1}{2}\sum_{i,j} N_i N_j (\pi R_i^2)(\pi R_j^2) \equiv \frac{1}{2}\sum_i N_i (\pi R_i^2) \sum_j N_j (\pi R_j^2) = \frac{1}{2} S_{e,1}^2. \tag{51}$$

We point out that the well known Austin-Ricket (AR) equation ($S = \frac{S_e}{1+S_e}$) is obtained by using Eq. (1) for $\beta = 2$. Its Taylor expansion is $S = \Sigma_{m=1}^{\infty} (-1)^{m-1} S_{e,1}^m$. It turns out that $S_{e,m} = S_{e,1}^m$, which compares with the KJMA solution where $S_{e,m} = \frac{1}{m!} S_{e,1}^m$. The question now arises about the possibility to justify the AR equation in the framework of the theory of phase transformation ruled by spatially correlated nucleation. On the basis of Eq. (37), the condition $S_{e,m} = S_{e,1}^m$ therefore implies

$$S_{e,1}^m = \frac{1}{m!} \sum_{i_1, i_2, \ldots, i_m} \int f_{i_1 i_2 \cdots i_m}^{(m)} \Omega_{i_1 i_2 \cdots i_m}^{(m)} d\mathbf{r}_{1,i_1} d\mathbf{r}_{2,i_2} \ldots .. d\mathbf{r}_{m,i_m}, \tag{52}$$

subjected to the constraint (f-function normalization)

$$\int f_{i_1 i_2 \cdots i_m}^{(m)} d\mathbf{r}_{1,i_1} d\mathbf{r}_{2,i_2} \cdots d\mathbf{r}_{m,i_m} = n_{i_1} n_{i_2} \cdots n_{i_m}, \tag{53}$$

where n_{i_k} denotes the number of dots. In addition

$$S_{e,1}^m = \sum_{i_1, i_2, \ldots, i_m} \int \Omega_{i_1 i_2 \cdots i_m}^{(m)} d\mathbf{r}_{1,i_1} d\mathbf{r}_{2,i_2} \ldots d\mathbf{r}_{m,i_m}. \tag{54}$$

At present we cannot demonstrate whether or not Eqs. (52)–(54) can be simultaneously satisfied by an appropriate set of $f^{(m)}$ distribution functions. If the answer were in the affirmative, the AR equation would imply the non-Poissonian distribution of nuclei as hypothesized in Ref. 43. Moreover, one has to bear in mind that a "repulsive" correlation among nuclei implies, as a function of $S_{e,1}$, a "faster" evolution than the KJMA kinetics. Since the AR equation evidences an opposite behavior, it would imply an "attractive" correlation.[30]

V. CONCLUSIONS

In conclusion, we have shown that Eq. (1) can be successfully applied for describing instantaneous cluster growth. The link between the phenomenological parameter β and the pair distribution function has been established. In this case the phenomenological equation is an excellent approximation for $\gamma_0 \cong 0.59$. The physical meaning of the impingement factor has been evidenced by means of a stochastic analysis based on the m-dot distribution functions. The same equation can be employed for modeling spatial correlated nucleation according to the hard-core model when both growth and nucleation rates are constant. Under these circumstances, the impingement factor is in the range $0.2 < \gamma < 0.3$. The connection between Avrami's set theory and the statistical thermodynamics of rigid disks has been established. Our analysis demonstrates that if the deviation between AR and KJMA kinetics are ascribed to correlation effects, then correlation has to be attractive.

APPENDIX

It is possible to show that scaling properties of the $Q(\Delta_X)$ probability also hold in the case of simultaneous nucleation of correlated nuclei according to hard-core model. Under these circumstances, nuclei cannot be at a distance shorter than R_{hc}. We recall that $Q(\Delta_X)$ is the probability that no nuclei are in the circle of radius X. The n-particle distribution functions can be written in the form $f_m = N^m \tilde{f}_m$, where $\tilde{f}_m$ is a function of the particle coordinates, hard-core radius (R_{hc}), and particle density (N). Since the quantity $f_m d\mathbf{r}_1 \cdots d\mathbf{r}_m$ is scaling invariant, the same property is satisfied by the $\tilde{f}_m$ functions. Therefore, for a homogeneous system, these functions are expected to be of the form $\tilde{f}_m(\frac{r_{12}}{R_{\mathrm{hc}}}, \ldots, \frac{r_{1m}}{R_{\mathrm{hc}}}, NR_{\mathrm{hc}}^2)$, where $r_{1j} = |\mathbf{r}_j - \mathbf{r}_1|$ are the relative coordinates. Moreover, through the change in variables $\mathbf{r}_i \to \frac{r_i}{X} \equiv \mathbf{r}_i'$, the integration domain in Eq. (5) is the unit circle and the Q expression becomes

$$Q(\Delta_X) = 1 + \sum_{m=1}^{\infty} \frac{(-1)^m}{m!} S_e^m \int_{\Delta_1} \tilde{f}_m\left(S^*, \frac{Xr_{12}'}{R_{hc}}, \ldots, \frac{Xr_{1m}'}{R_{hc}}\right) \times dr_1'^2 dr_{12}'^2 \cdots dr_{1m}'^2, \tag{A1}$$

where polar coordinates have been employed ($d\mathbf{r} = \pi dr^2$), $S_e = \pi N X^2$ is the extended surface, and $S^* = \pi N R_{\mathrm{hc}}^2$. Equation (A1) can be rewritten as

$$Q(\Delta_X) = 1 + \sum_{n=1}^{\infty} \frac{(-1)^n}{n!} h_n\left(S^*, \frac{S_e}{S^*}\right) S_e^n. \tag{A2}$$

For $X = R_{\mathrm{hc}}$ ($S_e = S^*$), the probability $Q(\Delta_X)$ is a function of S_e.

[1] A. N. Kolmogorov, U. R. S. S. Bull. Acad. Sci (Cl. Sci. Math. Nat) **3**, 355 (1937).
[2] M. Avrami, J. Chem. Phys. **7**, 1103 (1939); **8**, 212 (1940).
[3] W. A. Johnson and R. F. Mehl, Trans. Am. Inst. Min., Metall. Pet. Eng. **135**, 416 (1939).
[4] M. J. Starink, Int. Mater. Rev. **49**, 191 (2004).
[5] M. Fanfoni and M. Tomellini, J. Phys.: Condens. Matter **17**, R571 (2005).
[6] R. A. Ramos, P. A. Rikvold, and M. A. Novotny, Phys. Rev. B **59**, 9053 (1999).
[7] S. Jun and J. Bechhoefer, Phys. Rev. E **71**, 011909 (2005); S. Jun, H. Zhang, and J. Bechhoefer, *ibid.* **71**, 011908 (2005).
[8] V. I. Trofimov and H. S. Park, Appl. Surf. Sci. **219**, 93 (2003).
[9] B. Pacchiarotti, M. Fanfoni, and M. Tomellini, Physica A **358**, 379 (2005).
[10] M. P. Shepilov and D. S. Baik, J. Non-Cryst. Solids **171**, 141 (1994).
[11] M. P. Shepilov, Glass Phys. Chem. **30**, 291 (2004).
[12] D. Crespo and T. Pradell, Phys. Rev. B **54**, 3101 (1996).
[13] T. Pusztai and L. Granasy, Phys. Rev. B **57**, 14110 (1998).
[14] B. J. Kooi, Phys. Rev. B **70**, 224108 (2004).
[15] A. Korobov, Phys. Rev. B **76**, 085430 (2007).
[16] A. Almansour, K. Matsugi, T. Hatayama, and O. Yanagisawa, Mater. Trans., JIM **37**, 1595 (1996).
[17] D. P. Birnie III and M. C. Weinberg, J. Chem. Phys. **103**, 3742 (1995).
[18] A. A. Burbelko, E. Fraś, and W. Kapturkiewicz, Mater. Sci. Eng., A **413**, 429 (2005).
[19] M. Tomellini and M. Fanfoni, Phys. Rev. B **55**, 14071 (1997).
[20] P. Bruna, D. Crespo, R. Gomzalez-Cinca, and E. Pineda, J. Appl. Phys. **100**, 054907 (2006).
[21] N. X. Sun, X. D. Liu, and K. Lu, Scr. Mater. **34**, 1201 (1996).
[22] J. Farjas and P. Roura, Phys. Rev. B **75**, 184112 (2007).
[23] P. A. Mulheran and J. A. Blackman, Phys. Rev. B **53**, 10261 (1996).
[24] B. S. Lement and M. Cohen, Acta Metall. **4**, 469 (1956).
[25] M. Hillert, Acta Metall. **7**, 653 (1959).
[26] J. B. Austin and R. L. Rickett, Trans. Am. Inst. Min., Metall. Pet. Eng. **135**, 396 (1939).
[27] M. J. Starink, J. Mater. Sci. **36**, 4433 (2001).
[28] M. C. Bartelt, C. R. Stoldt, C. J. Jenks, P. A. Thiel, and J. W. Evans, Phys. Rev. B **59**, 3125 (1999).
[29] E. Bosco, J. Chem. Phys. **97**, 1542 (1992).
[30] P. R. Rios, J. C. P. T. Oliveira, V. T. Oliveira, and J. A. Castro, Mater. Res. **9**, 165 (2006).
[31] T. Tagami and S.-I. Tanaka, Acta Mater. **45**, 3341 (1997).
[32] E. Helfand, H. L. Frish, and J. L. Lebowitz, J. Chem. Phys. **34**, 1037 (1961).
[33] Y. C. Chiew and E. D. Glandt, J. Colloid Interface Sci. **99**, 86 (1984).
[34] M. Tomellini, M. Fanfoni, and M. Volpe, Phys. Rev. B **62**, 11300 (2000).
[35] P. Schaaf and J. Talbot, Phys. Rev. Lett. **62**, 175 (1989).
[36] J. W. Evans, Phys. Rev. Lett. **62**, 2642 (1989).
[37] N. V. Brilliantov, Y. A. Andrienko, P. L. Krapivsky, and J. Kurths, Phys. Rev. Lett. **76**, 4058 (1996).
[38] M. Manciu and E. Ruckenstain, Colloids Surf., A **232**, 1 (2004).
[39] E. L. Hinrichsen, J. Feder, and T. Jossang, J. Stat. Phys. **44**, 793 (1986).
[40] M. Fanfoni, M. Tomellini, and M. Volpe, Phys. Rev. B **65**, 172301 (2002).
[41] M. Tomellini, M. Fanfoni, and M. Volpe, Phys. Rev. B **65**, 140301(R) (2002).
[42] M. Fanfoni and M. Tomellini, Eur. Phys. J. B **34**, 331 (2003).
[43] R. A. Clemente and A. M. Saleh, Phys. Rev. B **65**, 132102 (2002).